Characterization of the Distributed Cavity Phase Shift in FO2 for Improving the Accuracy of SYRTE Fountain Clocks

J. Guéna[(1)], P. Rosenbusch[(1)], Ph. Laurent[(1)], M. Abgrall[(1)], D. Rovera[(1)], G. Santarelli[(1)], M. E. Tobar[(1)], R. Li[(2)], K. Gibble[(2)], S. Bize[(1)] and A. Clairon[(1)]

[(1)] LNE-SYRTE, Observatoire de Paris, UMR CNRS 8630, Paris, France
Email:jocelyne.guena@obspm.fr

[(2)] Department of Physics, The Pennsylvania State University, University Park, Pennsylvania 16802, USA

INTRODUCTION

The distributed cavity phase (DCP) shift is a significant source of uncertainty in the accuracy budget of several atomic fountains (see for instance [1-2]). This effect arises when the moving cold atom cloud interacts with the imperfectly stationary microwave field inside the Ramsey cavity. The effect depends on several parameters: The cavity geometry which determines the phase distribution in the cavity, the atomic cloud position and velocity distributions, the microwave power, the overall fountain geometry and the detection parameters which modify the effective velocity distribution of detected atoms. Due to this large number of parameters, there is no straightforward method to measure the distributed cavity phase shift in atomic fountains. So far, the related uncertainty has typically been estimated based on one of several available models for the phase distribution [3-6], on measurements of the atomic cloud parameters and their stability in time and on worst case calculations of the clock shift.
Here we present our new investigation of the problem using the SYRTE FO2 Cs/Rb fountain. Our approach is in three steps. First, we compute the 3-dimensional map of the cavity field from Maxwell's equations. Second, we use the 3D-field map as input into a Monte-Carlo simulation of the atomic response to calculate the frequency shift for any experimental configuration. Third, we measure clock frequency shifts in various experimental configurations for a large range of clock parameters, and compare with the model to estimate uncertainty. Importantly, this work addresses both odd terms (largely improving over our earlier work [7]) and even terms with respect to azimuthal symmetry, providing a stringent test of the model of [5]. The first section of this paper is a short reminder of the experimental set-up with focus on details relevant to the present work. The following section is devoted to the theoretical model comprising the computation of the cavity field and the Monte-Carlo simulation. Only the concepts and main ingredients are presented. The next section reports on measurements performed with FO2 and presents the comparisons with the model.

EXPERIMENTAL SETUP

An updated detailed description of the FO2 set-up is given in [1]. FO2 is running continuously as a dual Cs/Rb clock. Here we focus on the Cs part of FO2. The Rb counterpart is very similar. The FO2-Cs fountain operates with an optical molasses using six laser beams aligned in the (111) configuration and loaded from a 2D-MOT. In the present experiments a loading time of 500 ms was used. Atoms are launched upward with a velocity of 4.334 m.s-1 (apogee 0.957 m), cooled to ~0.8 μK and pass through a state selection microwave cavity. The F=3 $m_F = 0$ state is selected by adiabatic population transfer, and remaining atoms in F=4 non zero m_F states are pushed out by a dedicated laser beam.
During standard clock operation, the Ramsey interrogation probing the hyperfine transition consists of two microwave interactions separated by a free time of flight of 0.60 s. The resonator situated 0.518 m above the capture zone is a TE_{011} cylindrical cavity (diameter 50 mm, length 26.83 mm) made of copper walls with cut-off guides (inner diameter 12 mm, length 48 mm) at the two endcaps. The cavity can be fed fed either symmetrically or asymmetrically owing to two feedthroughs (inner diameter 5 mm) symmetrically placed at cavity midsection. The unloaded and loaded quality factors of the cavity are $Q_0 = 27800$ and $Q = 7000$ (cavity linewidth $\Gamma=\omega_0/Q= 2\pi\times1.3$ MHz), respectively. Tuning of the cavity occurs at 300 K. The microwave signal probing the atomic transition is synthesized from the ultra-stable signal provided by a cryogenic sapphire oscillator weakly phase-locked to a hydrogen maser. The synthesis includes a computer-controlled high-resolution digital synthesizer in order to tune the interrogation signal to the atomic transition. The synthesizer includes a Mach-Zehnder interferometer RF switch at 400 MHz (extinction ratio > 50 dB) [9]. The switch turns off the microwave signal when atoms are outside the microwave cavity with the purpose of suppressing possible microwave leakage during the Ramsey interrogation. It also allows us to interrogate the atoms with a single Rabi interaction, either at upward (Ramsey1) or at downward passage (Ramsey2) through the cavity. The synthesizer has two outputs with power and phase adjustments on one channel to provide symmetrical feeding of the Ramsey resonator. The detection zone consists of two separate standing waves of resonant light (the second one with repumper light) located (0.122 m and 0.136 m) below the molasses zone, allowing detection of the two clock states by induced fluorescence, from which the transition probability is calculated. The detection beams (Gaussian beam radius 8.6 mm at $1/e^2$) are truncated by a rectangular mask (vertical dimension 7 mm) and the hole of the Ramsey cavity determines the radial size (0.006 mm) of the detected cloud in the horizontal plane. The fluorescence light is collected onto two photodetectors during 100 ms. The detected atomic transition probabilities at each side of the Ramsey fringe determine

the frequency corrections applied via the synthesizer. These corrections are the basis for evaluating frequency stability and measuring frequency shifts. Typical clock instability is 3.5×10^{-14} @ 1 s limited by the present number of atoms.

THEORETICAL MODEL

Overview of the Computation of the Ramsey Field and and Relevant Frequency Shifts

The computation is based on the model by R. Li and K. Gibble [5] which uses the perturbation of the boundary conditions method. The first step is to solve the eigenfunctions and eigenvalues problem for perfect conducting walls providing the unperturbed fields $\vec{H}_0$ and $\vec{E}_0$ taking into account the holes at the endcaps. In a second step the effects of the lossy walls and of the feeds are computed, which gives rise to the perturbed fields

$$\vec{H} = \vec{H}_0 + (\alpha + i)\vec{g}\,;\ \vec{E} = \vec{E}_0 + (\alpha + i)\vec{f}\,. \qquad (1)$$

In (1) $\alpha = \Delta/\Gamma$ accounts for a possible cavity detuning Δ relative to the atomic frequency ω_0. $\Gamma = \omega_0/Q$ is the cavity linewidth. The Maxwell's equations define equations for the field perturbations $\vec{f}$ and $\vec{g}$. The boundary conditions (BC) on the copper walls are defined by the unperturbed field value on the walls and by the skin depth $\delta \propto 1/\sqrt{\sigma}$ where σ is the finite copper conductivity. BC are also added to account for the feeds. To realize this task, it is necessary to decompose the perturbed field $\vec{g}$ azimuthally in order to transform the hard 3D-problem into a tractable 2D numerical problem for each azymuthal component $\vec{g}_m$. Additionally, the atomic cloud travels near the cavity axis, in such a way that practically only the lowest order terms are relevant (m = 0,1,(2)).

In our experiment, we use three feeding configurations: two of them are "asymmetric" configurations where we feed either only from one side ("Asym1") or only from the other side ("Asym2") letting the unfeeded feedthrough loaded on 50 Ω by a microwave isolator. In an asymmetric feed configuration an energy flow is created through the cavity: $1/Q_2$ in Asym1, or $1/Q_1$ in Asym2. The fields in these two asymmetric configurations, for cavity tuned to resonance, are given by:

$$\vec{H}_1 = \vec{H}_0 + i(\vec{g}_{even} + \vec{g}_{odd}(1 + \frac{2Q_0}{Q_2}))$$

$$\vec{H}_2 = \vec{H}_0 + i(\vec{g}_{even} - \vec{g}_{odd}(1 + \frac{2Q_0}{Q_1}))$$

where $\vec{g}_{even}$ and $\vec{g}_{odd}$ refer to the sum of even and odd azymuthal components respectively. The g-odd contributions to the fields have opposite sign in the two asymmetric configurations (as expected for the power flow through the feeds), and they would be just opposite if the feeds were identical, namely if $1/Q_1 = 1/Q_2$. From the g's we get the frequency shifts in each configuration, denoted Asym1 and Aym2 respectively, or equivalently the differential and average shifts:

$$\text{Asym1-Asym2} \ \Leftrightarrow\ g_{odd} \times 2Q_0/Q, \ \text{with } 1/Q = 1/Q_0 + 1//Q_1 + 1//Q_2 \qquad (3)$$

$$(\text{Asym1+Asym2})/2 \ \Leftrightarrow\ g_{even} + g_{odd} \times Q_0 \times (1/Q_2 - 1/Q_1) \qquad (4)$$

In (3) Q is the Q-factor which accounts for all losses and which is measured experimentally. The differential shift (3) is the quantity used to probe g-odd. The average shift (4) has contribution from g-even, and also from g-odd but only if the couplings are not symmetric.

The third experimental case is the "symmetric" feed configuration consisting in feeding the cavity from both sides. In that case we adjust both phase and amplitudes of the two channels (we use the atoms as a probe) so as to realize a linear superposition of $\mathbf{H}_1$ and $\mathbf{H}_2$ with equal weights ½ (to better than 1%) and same phase (within 80 mrad). The frequency shift, denoted "Sym" in that case, is:

$$\text{Sym} \ \Leftrightarrow\ g_{even} + g_{odd} \times Q_0 \times (1/Q_2 - 1/Q_1), \qquad (5)$$

i.e. it should be just equal to the average shift (4):

$$\text{Sym} = (\text{Asym1} + \text{Asym2})/2 \qquad (6)$$

This relation can be checked experimentally as a test of the superposition of the fields. As an extended test, we allow for a phase imbalance ($2\varphi_1$) between the two feeds and also for non-zero cavity detuning Δ. Then the superposition relation (6) is modified and we find that there is an additional contribution to the shift Sym:

$$\text{Sym}(2\varphi_1) - \text{Sym}(0) \ \Leftrightarrow\ (g_{odd} \times 2Q_0/Q) \times \tan\varphi_1 \times (\Delta/\Gamma) \qquad (7)$$

Using (3) and (6), from (7) we get the following relation:

$$\frac{Sym(2\varphi_1) - (Asym1 + Asym2)/2}{(Asym1 - Asym2)} = \tan\varphi_1 \times \Delta/\Gamma \qquad (8)$$

which is easily tested experimentally. Indeed, this quantity depends only on the feeding phase imbalance and on the cavity detuning. Note that this simple, although not straightforward result can be derived in a much simpler model of a Fabry-Perot cavity fed from the two sides.

Monte-Carlo simulation

A further step to compare theory and experiment is to compute the effect of the perturbed field on the atomic response. This is done using a Monte-Carlo simulation. The inputs for this simulation are the computed maps of $\mathbf{H}_0$ and of the **g** components, the cloud parameters and the detection geometry. The initial cloud spatial distribution (Gaussian) used in the computation reproduces the measured distribution using a calibrated CCD camera image with absolute position reference with respect to the other fountain parts. The initial velocity distribution (Gaussian or Modified Lorentz) is based on the detected atom time of flight. The inhomogeneous detection response (Gaussian) is the convolution of the atomic response with the detection beam profile. After randomly choosing a trajectory according to these distributions, the program solves the time dependent Schrödinger equation for the 2-level atom. This leads to the determination of the transition probability for one atom. The program then averages over many trajectories taking into account the inhomogeneous detection response. With this the average transition probability can be computed for any sets of parameters. Note that this computation method has been compared to a second independent computation scheme using the sensitivity function [8]. For the same inputs, the two computations are in excellent agreement. To compare with the experiment we compute the perturbed transition probability due to the perturbed field on both sides of the Ramsey central fringe, P^+_{theory} , P^-_{theory}.
In the experiment, we perform usual frequency shifts measurements by locking to the line centre based on the difference in transition probabilities at mid-fringe. To compare with the simulation we use the measured frequency shift $\Delta\nu$ and the measured slope of the fringe at mid-fringe $dP/d\nu$ to compute the perturbed transition probability difference:

$$P^+_{exp} - P^-_{exp} = dP^+_{exp} - dP^-_{exp} = 2 \times (dP/d\nu) \times \Delta\nu \qquad (9)$$

EXPERIMENTS AND COMPARISON WITH THE THEORETICAL MODEL

Consistency of the model with the measured Rabi Oscillations

For consistency, the model should be able to reproduce the contrast of the Rabi oscillations at resonance. The transition probabilities for a single interaction (way up or way down), and for both simultaneously (Ramsey interrogation), were measured as a function of the microwave power up to field amplitudes corresponding to $11\times\pi/2$ pulse area for one interaction. The two Ramsey interactions have different sensitivity to the parameters: Ramsey1 is mostly sensitive to initial cloud distribution (size and position) while Ramsey2 is mostly sensitive to the velocity distribution and to the detection curvature. Using the values for the parameters: initial cloud size 3mm *rms*, width of initial velocity distribution 7.1 mm/s *rms* (corresponding to an initial cloud temperature of 0.8 µK), and detection curvature (response $\propto \exp[-(x/x_0)^2]$ with x_0 = 7 mm), determined as mentioned above, we obtain agreement between simulations and measured contrasts. These values are also used for the computation of P^+_{theory} and P^-_{theory} to compare with the frequency shifts measured in the same experimental conditions.

Measurements and Characterization of Odd Azymuthal Symmetry DCP effects

Microwave Power and Cloud Launch Direction Dependence
To be sensitive to the DCP m-odd components, we tilt the fountain table (which lies on three feets manually adjustable in height) and hence the launch direction (*z*-axis) with respect to gravity. As a result, we shift the centre of the atomic cloud between the first and the second Ramsey interactions. The tilt is performed either around the *x*-axis parallel to the feeding direction or around the y-axis perpendicular. Then we perform differential frequency shift measurements between the three feeding modes in interleaved configurations (lasting 50 fountain cycles) so as to eliminate long-term drifts. At a given tilt, measurements last between half a day and one day in order to reach a statistical resolution in the low 10^{-16} range.
Fig. 1 shows the results of the measurements of the differential shift "Asym1-Asym2" as a function of the tilt angle around y-axis for multiple $\pi/2$ Ramsey pulses. At a given microwave power, the dependence with the tilt angle is linear, as expected for small angles: the slope is $(6.02 \pm 0.15)\times10^{-15}$ /mrad for $\pi/2$-pulses. Dependence with pulse area, however, is not simple: there are changes both in sign and magnitude. Table 1 shows the comparison between the measured differential shifts "Asym1-Asym2", translated into change of transition probability (P^+ - P^-), and the

simulation, for a tilt angle of 1.6 mrad. We find agreement between experiment and theory. No significant dependence is observed when tilting around x-axis. Additionally, we verify that the linear superposition of the two fields from the two feeds is realized in the "symmetric" case, *i.e.* the measured shifts satisfy to (6). These results are consistent with our previous measurements [7]. In the present work the same measurements were performed simultaneously with FO2-Rb. The results are similar, up to an overall scaling factor of about ½.

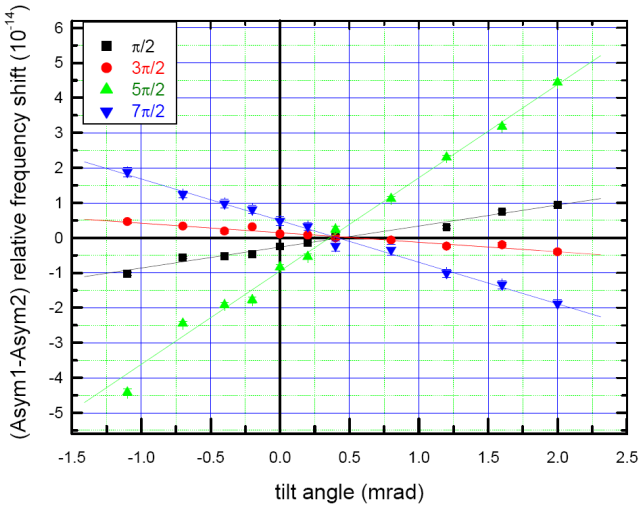

Fig. 1: Differential frequency shift (Asym1-Asym2) between the two asymmetric configurations *vs* tilt around y for multi-π/2 Ramsey pulses.

Table 1. Comparison between the measurements and the model for the differential frequency shift (Asym1-Asym2), translated into $P^+ - P^-$, for a tilt angle of 1.6mrad.

Pulse area (× π/2)	**Experiment** $P^+ - P^-$ (ppm)	**Model** (ppm)
1	346 ± 15	419
3	-110 ± 16	-122
5	955 ± 16	1025
7	-273 ± 17	-288
9	1113 ± 22	1130

For better characterization, further measurements are carried out by varying microwave amplitude in finer steps. The results will be published in a forthcoming paper.

Impact of phase imbalance and cavity detuning

The test of the impact of phase imbalance and cavity detuning as predicted by the model (8) was performed at a "large" tilt angle (1.6 mrad) to have non zero g-odd effects, and for π/2-pulses (corresponding differential frequency shift Asym1-Asym2 ≅ 10^{-14}). We change the feeding phase by $2\times\varphi_1$ in one channel, and readjust the microwave power equally in the two channels so as to keep the transition probability at resonance center unchanged (0.982). Again measurements are performed with the three interleaved configurations. Fig. 2 shows the results for the relevant quantity (8), *i.e.* the frequency difference between Sym and the average shift over Asym1 and Asym2, normalized by (Asym1-Asym2), as a function of the phase imbalance $2\varphi_1$. The three data sets corresponds to different values of the cavity detuning Δ (above, below and closed to cavity resonance), which was varied by heating the whole vacuum tube of FO2. The continuous lines are the fits to the data by the dependence $A \times \tan(\varphi_1) + b$, expected from (8). In this analysis, we had to allow for a small offset b ≅ -0.06 of technical origin which was identified and suppressed after the measurements. The fitted values A are consistent with the expected values Δ/Γ, as seen in Table 2. In these measurements, the frequency shift normalization by (Asym1-Asym2) was found independent of both the phase imbalance and detuning, as expected.

Table 1. Results of the fits to the data in Fig. 2.

Fitted A	Δ/Γ
0.367 ± 0.008	0.362
-0.271 ± 0.006	-0.24
0.033 ± 0.004	0.046

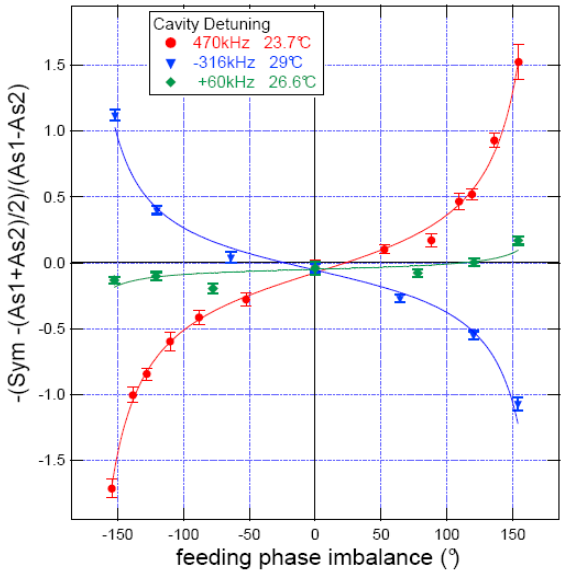

Fig. 2 : [Sym - (Asym1+Asym2)/2]/(Asym1-Asym2) *vs* feeding phase imbalance $2\varphi_1$ for three cavity detunings. Tilt angle 1.6 mrad and Ramsey π/2-pulses. Frequency shift normalization Asym1-Asym2 ≅ 10^{-14}. The continuous lines are the fitted curves with (8) .

Measurements and Characterization of even Azymuthal Symmetry DCP effects

So far frequency shifts associated with the g-even phase distribution had never been observed. Unlike the g-odd effects, there is no easy way to magnify them. Furthermore, there is no recourse to differential frequency shift measurements so one has to perform absolute frequency shift measurements. With a view to measure these shifts, g-odd effects are first minimized as well as possible by adjusting the symmetric feeding (phase and amplitude) and by adjusting the tilt angle (< 200 µrad) to cancel the (Asym1-Asym2) frequency difference. The shifts are expected to appear at high microwave power and have a specific dependence. The measurements are performed with FO2-Cs as a function of the microwave power, with frequency reference given either by FO2-Rb companion clock, or FO1 SYRTE fountain, operated both at nominal power. Fig. 3 shows the experimental results (black squares) and the comparison with the simulation. The red curve is the simulation (with g_0 term solely) without adjustment, while the blue curve is obtained by rescaling by the factor 1.5. As is conspicuous, the shape is well reproduced but a rescaling factor of 1.5 is required to obtain full agreement. A possible explanation for this mismatch is that the value we take for the wall surface conductivity (we take that of bulk copper) is too large. The impact of an asymmetry between the couplings is under current investigation, as well as contribution from g_2 term. Note finally that the relative frequency shift predicted at nominal power (π/2-pulses) is $\Delta\nu/\nu_0 = 4\times10^{-18}$ (6×10^{-18} if we rescale), *i.e.* negligible.

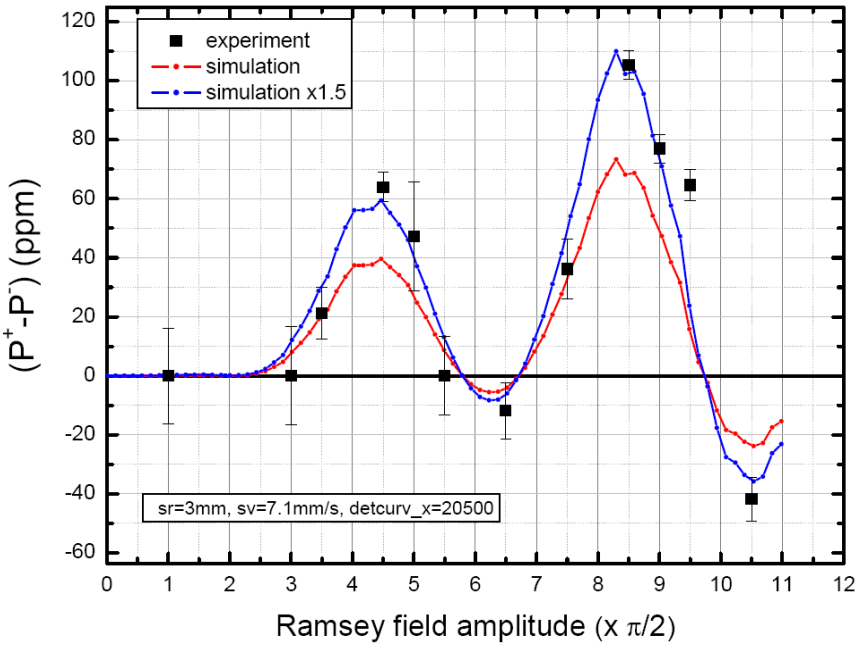

Fig. 3 : Absolute frequency shifts measured with FO2-Cs *vs* the microwave amplitude in unit of π/2-pulses for one interaction (Rabi frequency of 44.6 Hz at cavity centre). The shifts are translated into (P^+-P^-) expressed in ppm. The simulation is performed using the same values for the parameters as used in previous simulations (Rabi oscillations and g-odd effects).

CONCLUSION AND PERSPECTIVES

We have presented a quantitative comparison between measurements and an *ab-initio* model of Distributed Cavity Phase shifts in a fountain clock. For the first time both odd- and even- azimuthal components in the phase distribution are demonstrated and characterized. The experiment mostly validates the theoretical model of [5] opening the way to reduce uncertainty at 10^{-16}. This works has led us to reconsider our symmetrization procedure in order to account for a possible asymmetry of the coupling feeds. Work is in progress to elucidate the imperfect agreement between theory and experiment for the g-even term. In that respect, future measurements of absolute frequency shifts at large tilt angle should provide us with valuable information. The model can now be easily adapted to FO2-Rb, FO1 and FOM SYRTE fountains. Interestingly, cavity aspect ratios and Q-factors differ notably between them. Note that a measurement of the g-even term was reported simultaneously at this 2010 EFTF conference by V. Gerginov et al. from PTB.

REFERENCES

[1] J. Guéna et al., "Demonstration of a Dual Alkali Rb/Cs Fountain Clock", *IEEE Trans. on UFFC 2010*, 57, vol.3, pp. 647-653, March 2010; J. Guéna et al., "First dual mode operation of the Cs/Rb FO2 double fountain at SYRTE", *Proceedings of the 2009 EFTF-IFCS joint conference*, pp. 764-768 (2009).

[2] V. Gerginov, N. Nemitz, S. Weyers, R. Schröder, D. Griebsch and R. Wynands., "Uncertainty evaluation of the caesium fountain clock PTB-CSF2 ", *Metrologia* 47, pp. 65-79, 2010.

[3] A. Khursheed, G. Vecchi, and A. De Marchi, "Spatial variations of field polarization and phase in microwave cavities: application to the cesium fountain cavity", *IEEE Trans. Ultrason. Ferroelect. Freq. Contr.*, 43 (2), pp. 201-210, 1996.

[4] R. Schröder and U. Hübner and D. Greibsch, "Design and realization of the microwave cavity in the PTB caesium atomic fountain clock CSF1", *IEEE Trans. Ultr. Ferr. Freq. Contr.*, 49 (3), pp. 383–392, 2002.

[5] R. Li and K. Gibble, "Phase variations in microwave cavities for atomic Clocks", *Metrologia* 41, pp. 376-386, 2004; R. Li and K. Gibble, *Proceedings of the 2005 Frequency Control Symposium*, p 99, 2005.

[6] S.R. Jefferts, J.H. Shirley, N. Ashby, E.A. Burt, and G.J. Dick, "Power dependence of distributed cavity phase-induced frequency biases in atomic fountain frequency standards", *IEEE Trans. Ultrason. Ferroelect. Freq. Contr.*, 52 (12), pp. 2314-2321, 2005.

[7] F. Chapelet et al., "Investigation of the distributed cavity phase shift in an atomic fountain", *Proceedings of the 20th European Freq. and Time Forum*, Braunschweig, Germany, 2006.

[8] G. Santarelli, C. Audoin, A. Makdissi, Ph. Laurent, G. J. Dick, and A. Clairon, “Frequency Stability Degradation of an Oscillator Slaved to a Periodically Interrogated Atomic Resonator”, *IEEE Trans. Ultrason. Ferroelect. Freq. Contr.*, 45, pp. 887-894, 1998.
[9] G. Santarelli et al., “Switching atomic fountain clock microwave interrogation signal and high-resolution phase measurements”, *IEEE Trans. Ultrason. Ferroelect. Freq. Contr.*, vol. 56 (7), pp. 1319–1326, 2009.